journal

J. Am. Ceram. Soc., 86 [4] 717–26 (2003)

High-Temperature Neutron Diffraction of the $AlN–Al_2O_3–Y_2O_3$ System

Mamoun Medraj

Department of Mechanical Engineering, Concordia University, Montreal, Quebec, Canada

Robert Hammond

Neutron Program for Materials Research, National Research Council of Canada, Chalk River, Ontario, Canada

William T. Thompson

Department of Chemical Engineering, Royal Military College, Kingston, Ontario, Canada

Robin A. L. Drew*

Department of Metals and Materials Engineering, McGill University, Montreal, Quebec, Canada

The importance of aluminum nitride (AlN) stems from its application in microelectronics as a substrate material due to high thermal conductivity, high electrical resistance, mechanical strength and hardness, thermal durability, and chemical stability. Yttria (Y_2O_3) is the best additive for AlN sintering. AlN densifies by a liquid-phase mechanism, where the surface oxide, Al_2O_3, reacts with Y_2O_3 to form an Y-Al-O-N liquid that promotes particle rearrangement and densification. Construction of the phase relations in this multicomponent system is essential for optimizing the properties of AlN. The ternary phase diagram of the $AlN–Al_2O_3–Y_2O_3$ was developed by Gibbs energy minimization using interpolation procedures based on modeling the binary subsystems. This paper aims at testing the resultant understanding experimentally at selected compositions using *in situ* high-temperature neutron diffractometry. These experimental results agree with the thermodynamic calculations of $AlN–Al_2O_3–Y_2O_3$. The ternary phase diagram has been constructed for the first time in this work. High-temperature neutron diffractometry has permitted real time measurement of the reactions involved in this ternary system, especially to determine the temperature range for each reaction, which would have been difficult to establish by other means.

I. Introduction

ALUMINUM NITRIDE is being intensively studied as a suitable material for production of hybrid integrated circuit substrates because of its high thermal conductivity, high flexural strength, and nontoxic nature.[1] Sintering of AlN with the addition of Y_2O_3 occurs in the presence of liquid phase. During this process the interaction between Y_2O_3 and the surface oxide of AlN powder leads to the formation of a liquid.[2] The amount of liquid and the phase evolution at a selected sintering temperature can be better understood using equilibrium diagrams. Hence one can clearly see the importance of a detailed and complete study of the $AlN–Al_2O_3–Y_2O_3$ phase equilibrium.

To date, there is little information on the ternary $AlN–Al_2O_3–$ sintering additive systems.[3] Huseby *et al.*[4] reported a composition diagram showing the subsolidus phase equilibria in the $AlN–YN–Al_2O_3–Y_2O_3$ system and is very similar to that reported by Schuster.[5] Although this diagram consists of tie lines connecting the AlN corner with the intermediate compounds occurring on the $Al_2O_3–Y_2O_3$ side; however, no details are mentioned about its construction. Sun *et al.*[6] determined the subsolidus phase relationships and the isothermal section at 1850°C in the system Y-Al-O-N.

No effort has been made thus far in modeling and analysis of the entire $AlN–Al_2O_3–Y_2O_3$ system experimentally. The effect of Al_2O_3 additions on the phase reaction of the $AlN–Y_2O_3$ system at high temperatures of 1900° and 1950°C was investigated by Kim *et al.* They found that in the AlN–3 wt% Y_2O_3 system, $Al_2O_3{\cdot}0.2Y_2O_3$, YAM phase, with the lowest Al_2O_3 content of the yttrium aluminates was identified. And in the AlN–10 wt% Y_2O_3 system, unreacted Y_2O_3 was detected in addition to YAM, because the Y_2O_3 was in excess of the amount required for the YAM formation with the surface oxide.[7] In a very recent study, Boey *et al.*[8] studied Al_2O_3–20 wt% $AlN–5Y_2O_3$ composition and reported X-ray diffraction and SEM results in relation to thermal conductivity measurements for samples sintered at different temperatures.

In a ternary component system A–B–C, the other binary systems A–B, A–C, and B–C contribute similarly to the thermodynamic properties of the three-component system;[9] in our case they are $AlN–Al_2O_3$, $AlN–Y_2O_3$, and $Al_2O_3–Y_2O_3$, respectively. Binary diagrams of $Al_2O_3–Y_2O_3$, $AlN–Al_2O_3$, and $AlN–Y_2O_3$ were thermodynamically modeled. The obtained Gibbs energies of components, stoichiometric phases, and solution parameters were used for the calculation of isothermal sections and the liquidus surface of the $AlN–Al_2O_3–Y_2O_3$ system. A detailed description of the modeling of this system is published in previous work.[10] The predicted ternary phase diagram was verified experimentally using *in situ* high-temperature neutron diffractometry. The major advantage of neutron diffraction compared with other diffraction techniques is the extraordinary penetrating nature of the neutrons, which leads to its use in measurements under special environments.[11]

II. Experimental Procedure

To determine the phase evolution in the $AlN–Al_2O_3–Y_2O_3$ system, the neutron diffraction patterns were monitored *in situ* at elevated temperature using the DUALSPEC high-resolution

T. M. Besmann—contributing editor

Manuscript No. 187514. Received August 20, 2001; approved December 11, 2002.
Supported by NSERC Strategic Project Grant.
*Member, American Ceramic Society.

Table I. Chemical Composition of the Studied Samples

Sample no.	Composition (mol%) AlN	Al_2O_3	Y_2O_3
1	12	74	14
2	17.5	64	18.5
3	24	70	6
4	7	33	60
5	33	20	47

powder diffractometer, C2, at the NRU reactor of Atomic Energy of Canada Limited (AECL), Chalk River Laboratories. The diffractometer is an 800-channel position-sensitive detector that spans 80° in scattering angle, 2θ. The wavelength, λ, of the neutron beam was calibrated by measuring the diffraction pattern of a standard powder of alumina, obtained from the National Institute of Standards and Technology. λ = 1.33(1) Å and 2θ range from 8° to 88° were used in this experiment.

The diffractometer was equipped with a tantalum-element vacuum furnace capable of reaching temperatures as high as 2000°C. The furnace programming and data acquisition system were fully computerized, allowing accurate temperature control and rapid data collection.

AlN (grade F, supplied by Tokuyama Soda, Japan), Y_2O_3 powder (grade 5600, supplied by Union Molycorp, U.S.A., with 99.99% purity), and Al_2O_3 powder (grade A16-SG, supplied by Alcoa Industrial Chemical Division, Canada, with 99.8 purity) were mixed in various stoichiometric amounts. Table I and Fig. 1 show the composition of these samples. The premixed compositions were ball-milled in a plastic container for 24 h using 4 mm diameter Al_2O_3 media and reagent-grade isopropyl alcohol with a solid-to-liquid ratio of 1:5 by volume. The mixtures were dried in a microwave oven to completely remove the isopropyl alcohol. After drying, the mixtures were granulated through a 60 μm mesh sieve to create a fine powder mixture. A portion of each composition was encapsulated in molybdenum foil to prevent the powder from spreading in the sample chamber on evacuation, and to protect the apparatus when the sample melts.

After centering the furnace in the beam of the neutron diffractometer, the sample capsule was placed in a molybdenum pencil tube, which was located inside the furnace chamber. The aluminum furnace chamber was sealed, and the volume between the molybdenum tube and inside of the furnace chamber was evacuated to 10^{-8} atm. A neutron diffraction spectrum for each sample was collected at room temperature to form the reference for any reactions taking place on heating. The samples were heated while flowing nitrogen gas to prevent the decomposition of AlN. According to the recent study of D'yachkov *et al.* the decomposition of AlN was suppressed by nitrogen at atmospheric pressure.[12] The sample was observed *in situ* during heating and cooling. Neutron diffraction spectra were collected at incremental intervals until the spectra displayed loss of crystallinity or reached the maximum temperature of the furnace (2000°C). Then cooling started and neutron spectra were collected at incremental cooling temperatures to observe the precipitation of crystalline phases. The temperature was increased incrementally to closely follow the evolution of the reactions. At each step the temperature was maintained for 120 min to ensure that the reaction was complete. Since the furnace containing the sample was scanned, the acquired neutron diffraction spectra included peaks of the sample and those of the furnace. Correction of these spectra was achieved by subtracting the furnace peaks. For this purpose, neutron diffraction spectra were collected for the empty furnace at all of the temperatures of interest.

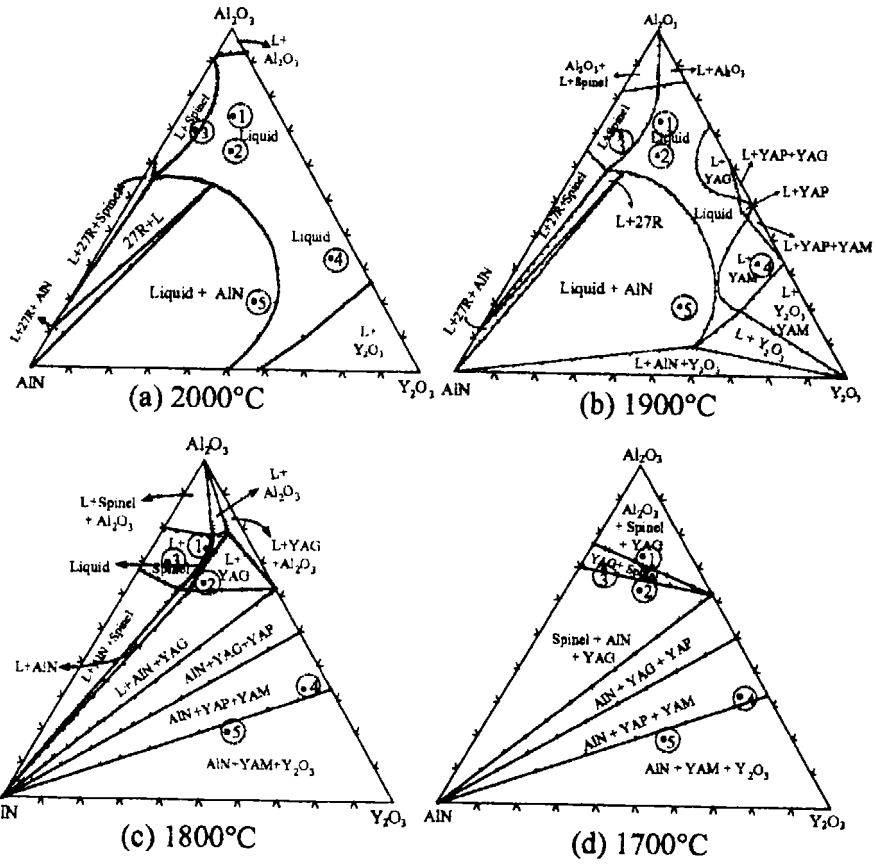

Fig. 1. AlN–Al_2O_3–Y_2O_3 isothermal sections at different temperatures with the five investigated ternary compositions.

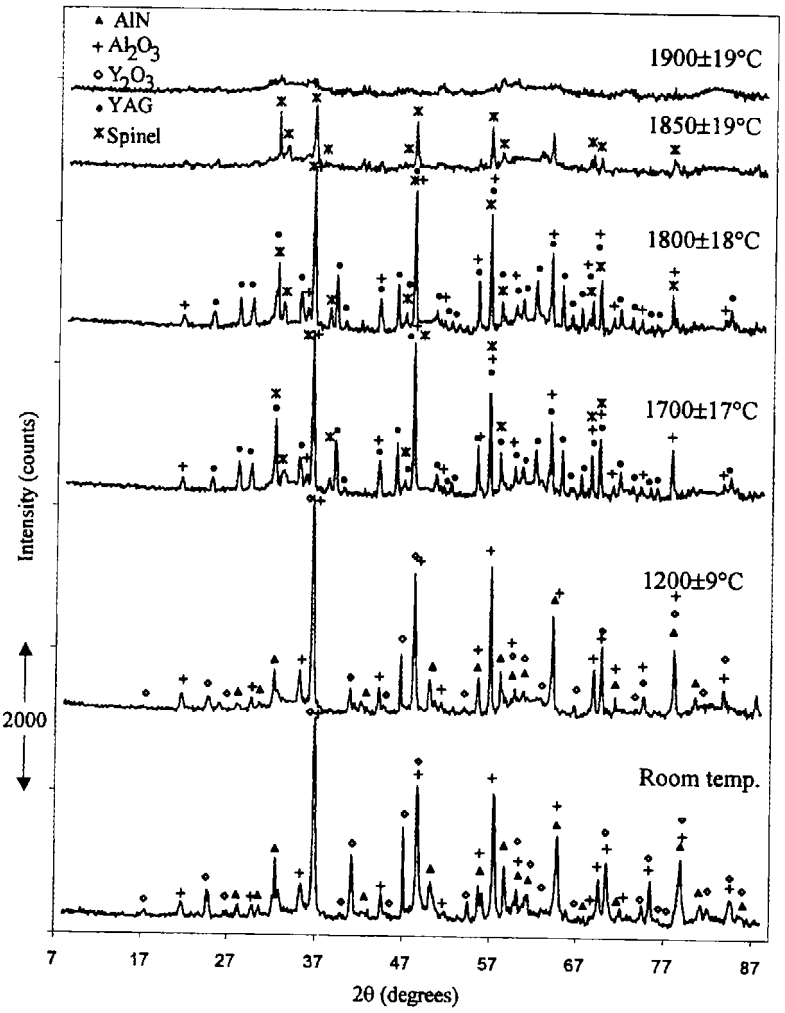

Fig. 2. Neutron diffractograms during heating of composition 1 (12 mol% AlN, 74 mol% Al_2O_3, and 14 mol% Y_2O_3).

III. Results

In this section, the experimental investigation of the AlN–Al_2O_3–Y_2O_3 ternary system will be discussed. Five different ternary samples, with compositions listed in Table I, were studied *in situ* at elevated temperature by neutron diffractometry. These compositions along with AlN–Al_2O_3–Y_2O_3 isothermal sections calculated at different temperatures are shown in Fig. 1. It can be seen from this figure that these compositions were carefully selected to be close to the phase boundaries to critically verify the predicted phase equilibrium. In this paper four compositions will be discussed.

The evolution of phase changes as a result of temperature increase was followed by acquiring neutron diffraction data for 120 min at selected temperature steps. Also cooling was conducted incrementally to detect the crystallization as well as the stability of each phase. Heating and cooling profiles were determined for each sample according to critical points, which were predicted from the thermodynamic calculations.

Diffraction patterns obtained during heating and cooling of each sample are shown in the following figures. The patterns are shifted by a suitable offset for better comparison. The temperature is presented with the uncertainty in the thermocouple measurement. The peaks are identified by markers given in the legend of each figure, and will be discussed and compared in conjunction with the thermodynamic findings in this section. The effect of thermal expansion was observed in all of the samples, with the peaks shifting to lower and higher diffraction angles due to heating and cooling, respectively.

(1) Composition 1

The reaction of this composition (12 mol% AlN, 74 mol% Al_2O_3, and 14 mol% Y_2O_3) during heating from room temperature to 1900°C is illustrated in Fig. 2. Detailed discussion of this composition is presented in Ref. 10. AlN peaks were identified as a hexagonal unit cell (space group *P6-3mc*, a = 3.112(0) Å and c = 4.978(0) Å), while Al_2O_3 peaks and Y_2O_3 peaks were identified using a rhombohedral unit cell (space group $R\bar{3}c$, a = 4.759(0) and c = 12.992(0))[13] and cubic unit cell (space group *Ia*3, a = 10.608(7) Å),[14] respectively.

The first changes are visible when comparing the neutron diffraction patterns at 1200°C and that at 1700°C, where additional peaks appear. The new peaks were found to belong to YAG ($5Al_2O_3{\cdot}0.3Y_2O_3$) and γ-spinel phases. YAG peaks were indexed as a cubic unit cell (space group *Ia3d*, a = 12.016(3) Å)[15] and γ-spinel peaks were indexed as a cubic unit cell (space group *Fd3m*, a = 7.9435(2) Å).[16,17] Unlike Al_2O_3 diffraction peaks, Y_2O_3 peaks were not observed at 1700°C; this means that all of the Y_2O_3 reacted to produce YAG phase. This is consistent with the ternary phase diagram shown in Fig. 1(d) where composition 1 lies in the three-phase region of Al_2O_3, γ-spinel, and YAG.

At 1850°C YAG peaks were not observed, whereas γ-spinel peaks were present. Since no other peaks were present at this temperature, it can be concluded that liquid formation started between 1800 ± 18° and 1850 ± 19°C, which is consistent with the isothermal section calculated at 1800°C and shown in Fig. 1(c). It can be seen from Fig. 2 that this composition had melted

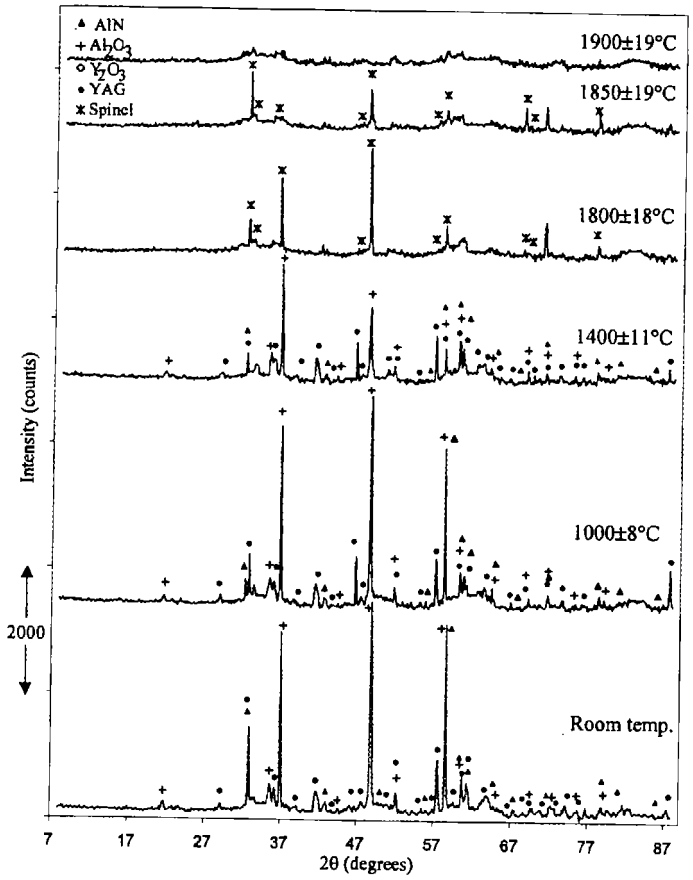

Fig. 3. Neutron diffractograms during cooling of composition 1 (12 mol% AlN, 74 mol% Al_2O_3, and 14 mol% Y_2O_3).

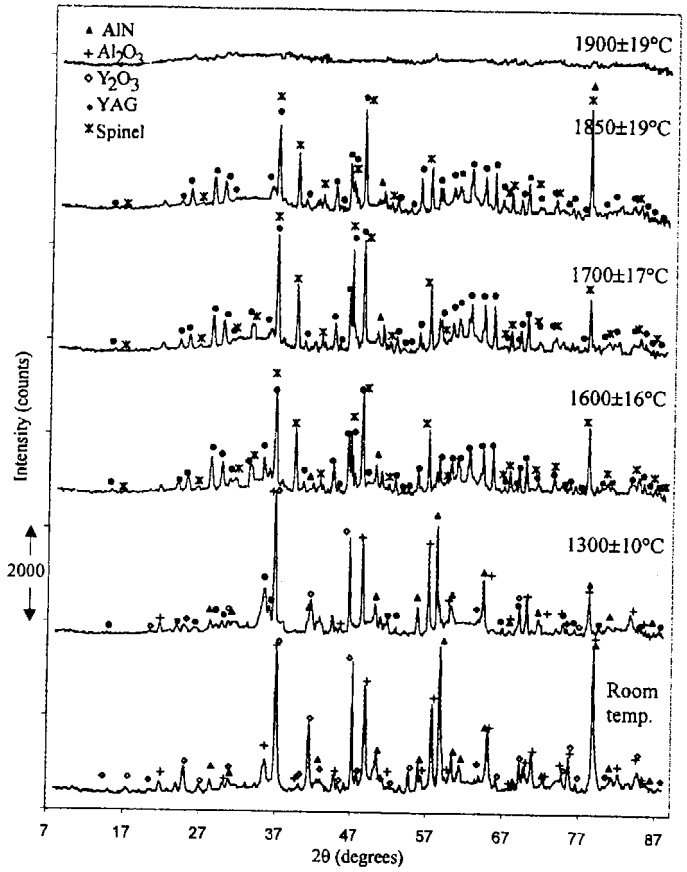

Fig. 4. Phase assemblage diagram of composition 1 (12 mol% AlN, 74 mol% Al_2O_3, and 14 mol% Y_2O_3).

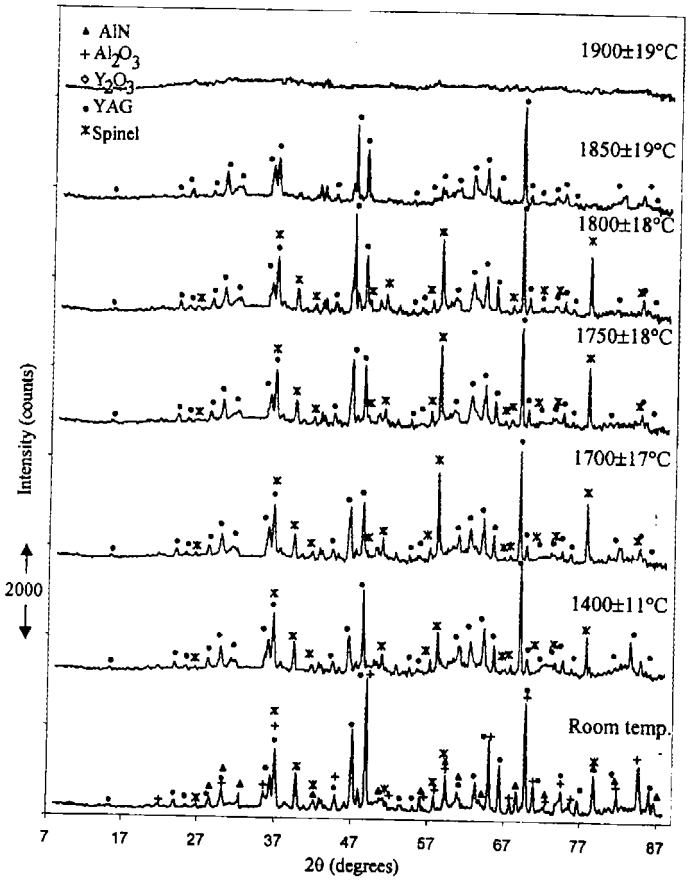

Fig. 5. Neutron diffractograms during heating of composition 2 (17.5 mol% AlN, 64 mol% Al_2O_3, and 18.5 mol% Y_2O_3).

between 1850° and 1900°C. This is consistent with the calculated isothermal section at 1900°C shown in Fig. 1(b).

Figure 3 shows the cooling cycle for composition 1. It can be seen that γ-spinel was fully crystallized at 1850°C, confirming that the solidification occurs between 1900° and 1850°C. On cooling to 1400°C, decomposition of the γ-spinel phase occurred and is evident by the appearance of new peaks of AlN and Al_2O_3. YAG peaks were also observed in the diffraction pattern collected at 1400°C. This sample is composed of AlN, YAG, and Al_2O_3 at room temperature.

(2) Composition 2

Different types of reactions were observed (Fig. 4) when starting with 17.5 mol% AlN, 64 mol% Al_2O_3, and 18.5 mol% Y_2O_3. The first changes are visible when comparing the neutron diffraction patterns collected at 1300°C with that at room temperature. The pattern at 1300°C clearly shows the reduction in the intensity of Y_2O_3 and Al_2O_3 peaks in addition to the growth of YAG peaks with no changes being observed in AlN content. YAG peaks continue to grow, whereas the peaks of Al_2O_3 and Y_2O_3 disappear with increasing temperature up to 1600°C. Moreover, traces of AlN can be observed along with γ-spinel and YAG. The patterns acquired in the temperature range of 1600° to 1850°C appear quite similar.

The isothermal section in Fig. 1(c) shows that this composition should form only liquid and YAG at 1800°C. However, peaks for γ-spinel were observed at 1850°C, indicating that no decomposition of γ-spinel took place during heating from 1700° to 1850°C. Figure 4 shows that this composition completely melted between 1850° and 1900°C. This is in agreement with the isothermal section calculated at 1900°C, where this composition lies in the liquid region (Fig. 1(b)).

Figure 5 shows the cooling cycle of composition 2. It can be seen that YAG was fully crystallized and in equilibrium with the liquid on cooling to 1850°C and neither AlN nor γ-spinel peaks were observed at this temperature. On cooling to 1800°C γ-spinel peaks begin to appear, indicating that γ-spinel crystallizes between 1850° and 1800°C. No differences were observed in the diffraction patterns after cooling to 1750°, 1700°, and 1400°C and AlN was not observed in any of these patterns. In addition to YAG and γ-spinel, Al_2O_3 and AlN were observed on cooling to room temperature. This confirms the decomposition of the γ-spinel phase to AlN and Al_2O_3 when cooling below 1400°C. Traces of the γ-spinel were observed at room temperature, suggesting incomplete decomposition of this phase. This might be due to the rapid cooling from 1400°C to room temperature without annealing at an intermediate temperature, as done for composition 1.

(3) Composition 3

Diffraction patterns of heating and cooling of composition 3 (24 mol% AlN, 6 mol% Al_2O_3, and 70 mol% Y_2O_3) are shown in Figs. 6 and 7, respectively. From Fig. 6 this composition formed YAG and γ-spinel phases at 1700°C, which is consistent with the isothermal section calculated at this temperature and shown in Fig. 1(d). As predicted thermodynamically, this composition forms liquid and γ-spinel at both 1900° and 2000°C, as shown in Figs. 1(b) and (a), respectively. Neutron diffraction patterns obtained at these two temperatures are in agreement with these predictions, showing γ-spinel as the only solid phase.

The first changes are visible when comparing the neutron diffraction patterns at 1500°C with that at room temperature, where additional peaks of YAG phase appear. YAG peaks continue to grow on increasing the temperature to 1700°C, indicating incomplete formation of the YAG at 1500°C. Also, AlN and Al_2O_3 were observed at 1500°C and disappeared at 1700°C to form γ-spinel.

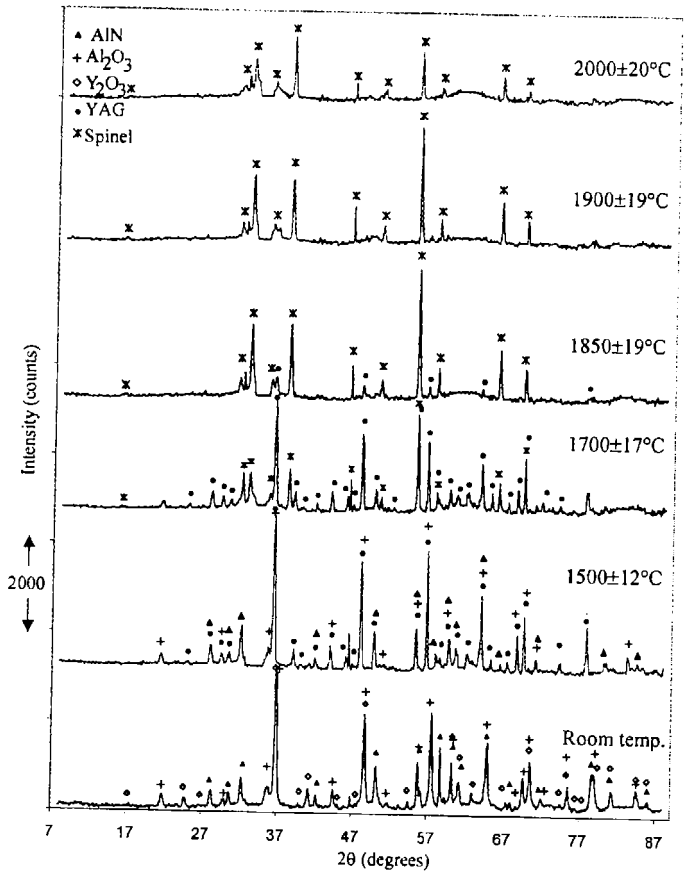

Fig. 6. Neutron diffractograms during cooling of composition 2 (17.5 mol% AlN, 64 mol% Al_2O_3, and 18.5 mol% Y_2O_3).

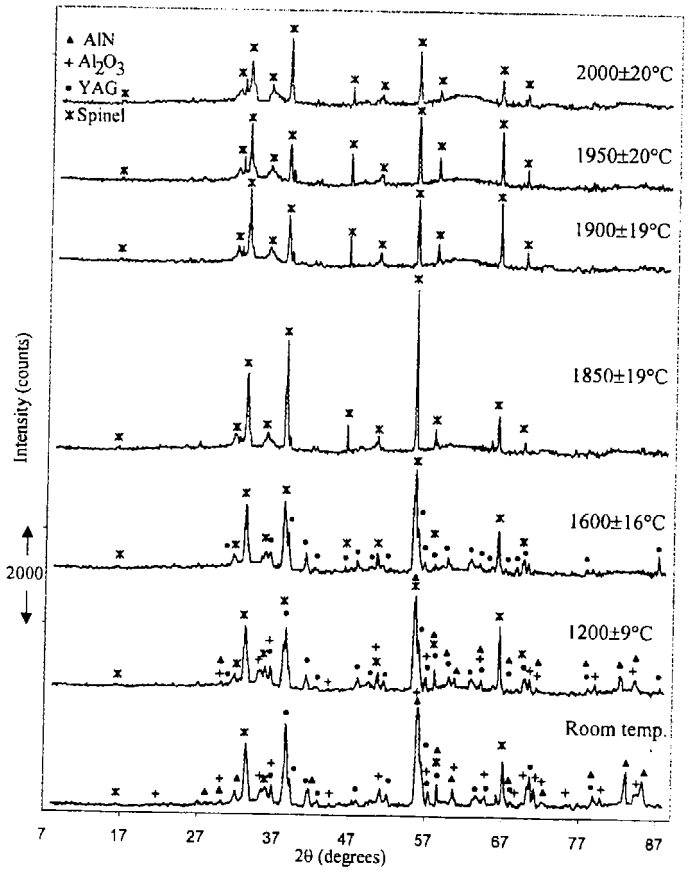

Fig. 7. Phase assemblage diagram of composition 2 (17.5 mol% AlN, 64 mol% Al_2O_3, and 18.5 mol% Y_2O_3).

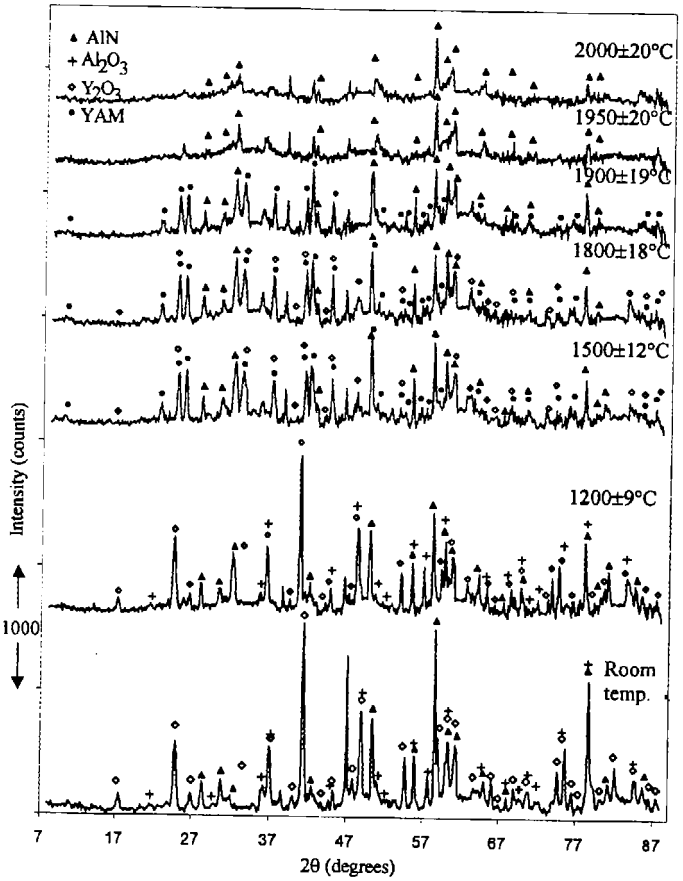

Fig. 8. Neutron diffractograms during heating of composition 3 (24 mol% AlN, 70 mol% Al_2O_3, and 6 mol% Y_2O_3).

By heating to 1850°C, most of the YAG peaks were eliminated; however, some weak peaks are observed, suggesting that traces of YAG still exist in conjunction with liquid and γ-spinel at this temperature. Thermodynamic calculations indicate that liquid and γ-spinel are the only equilibrium phases at 1850°C as shown in Fig. 12. The appearance of traces of YAG at this temperature may be because of slow reaction kinetics. Figure 7 supports this argument since no YAG peaks are observed on cooling to 1850°C. The neutron diffraction pattern collected at 1900°C shows only γ-spinel peaks, which indicates that the remaining material was a liquid. The γ-spinel peaks are weaker at 2000°C, indicating a small quantity of this phase and an increasing amount of liquid. The liquidus of this composition is higher than 2000°C, since γ-spinel is still present.

Figure 7 shows the neutron diffraction patterns acquired during the cooling of this composition. γ-Spinel is the only solid phase observed, and liquid coexists with γ-spinel down to 1850°C. The γ-spinel peak heights increase with decreasing temperature, showing increasing precipitation of this phase. This is in agreement with the thermodynamic calculations presented in Figs. 1(a–c), where this composition consists of only liquid and γ-spinel at 2000°, 1900°, and 1800°C. On cooling to 1600°C, YAG peaks appear and crystallize in the temperature range from 1850° to 1600°C. This is in agreement with the calculated phase diagram (Fig. 1(d)). At 1200°C, AlN and Al_2O_3 peaks were detected in addition to γ-spinel and YAG. This shows that γ-spinel decomposition occurred between 1600° and 1200°C. Since γ-spinel peaks were still present, incomplete decomposition of this phase occurred during cooling to 1200°C. The pattern acquired at room temperature shows a phase assemblage similar to that at 1200°C but with stronger AlN peaks and weaker γ-spinel peaks. This further confirms incomplete decomposition of γ-spinel phase under these experimental conditions and shows that the composition has not reached equilibrium for kinetic reasons.

(4) Composition 5

The development of the phase assemblage with increasing temperature up to 2000°C for composition 5 (33 mol% AlN, 20 mol% Al_2O_3, and 47 mol% Y_2O_3) is shown in Fig. 8. Comparing the neutron diffraction patterns at 1200°C and those at room temperature shows that no reaction occurred up to 1200°C. The first noticeable change for this sample was observed by comparing the neutron diffraction patterns collected at 1500° and 1200°C. Additional peaks of the YAM (Al_2O_3·0.2Y_2O_3) phase appear, whereas no traces of Al_2O_3 were observed at 1500°C, indicating complete reaction and formation of YAM phase. YAM peaks were identified as a monoclinic unit cell (space group $P2_1/c$, a = 7.4706(5) Å, b = 10.535(6) Å, c = 11.1941(8) Å, β = 108.888°(5)).[18] At this temperature significant amounts of AlN and Y_2O_3 were observed. Diffraction patterns of 1800° and 1500°C are practically unchanged, indicating that there is no reaction between AlN and YAM or Y_2O_3. This agrees very well with the isothermal sections show in Figs. 1(c) and (d) where this composition is in the three-phase region AlN, YAM, and Y_2O_3 at 1800° and 1700°C, respectively.

By heating to 1900°C, the Y_2O_3 peaks were eliminated, unlike YAM peaks which were still present, but Fig. 1(b) shows that this composition should have only AlN as a solid phase in equilibrium with the liquid phase, which is the composition observed in the neutron diffraction pattern collected at 1950°C instead. The phase assemblages found at 1950° and 2000°C are practically identical and are in agreement with the isothermal section calculated at 2000°C, and shown in Fig. 1(a).

On cooling from 2000° to 1900°C (Fig. 9), YAM appears in addition to AlN and indicates that YAM starts to recrystallize

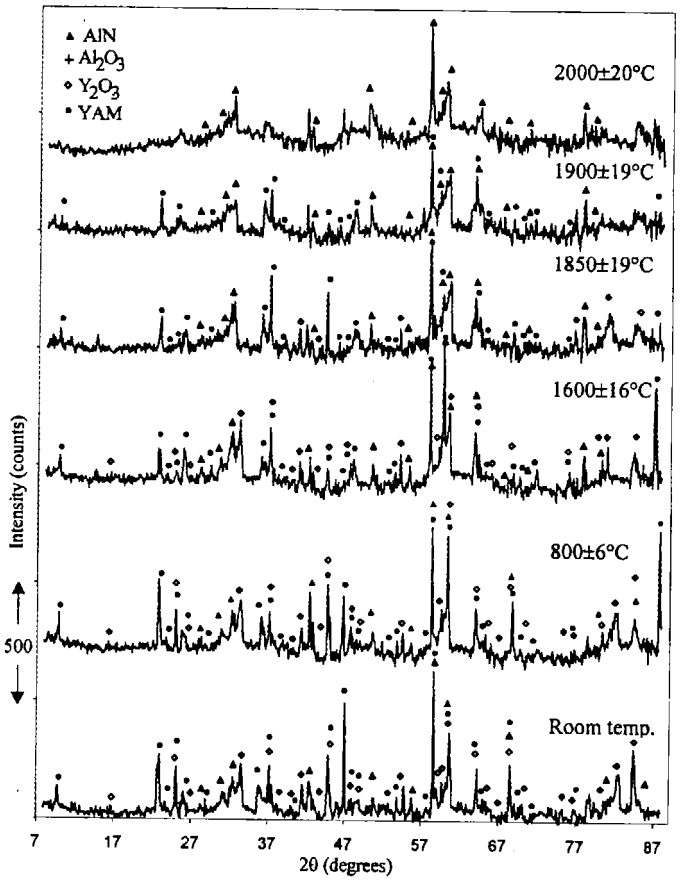

Fig. 9. Neutron diffractograms during cooling of composition 3 (24 mol% AlN, 70 mol% Al_2O_3, and 6 mol% Y_2O_3).

between 1900° and 2000°C. Further cooling to 1850°C resulted in formation of Y_2O_3 and further crystallization of YAM and AlN. The same phases were observed at 1600°C with changes in their relative amounts. These results agree very well with the neutron diffraction patterns acquired during heating as well as the isothermal sections presented in Fig. 1. On cooling to 800°C and then to room temperature, no difference was observed except an increase in the peak heights showing improved crystallization with decreasing temperature. At room temperature this composition consisted of AlN, YAM, and Y_2O_3 and again is consistent with the predicted phase diagram.

IV. Discussion

The *in situ* neutron diffraction experiments provide experimental evidence of formation, decomposition, and melting of each phase. Hence, the relative mass of each phase versus temperature is drawn, for the compositions in question, and compared with the results of neutron diffraction experiments.

Figure 10 is calculated from the thermodynamic database of AlN–Al_2O_3–Y_2O_3, for composition 1 (12 mol% AlN, 74 mol% Al_2O_3, and 14 mol% Y_2O_3). The proportion of each phase can easily be read from this figure. For instance, at 1700°C, 100 g of the overall material consists of 40 g of γ-spinel, 50 g of YAG, and 10 g of Al_2O_3. This is consistent with the diffraction data collected at 1700°C for this composition (Fig. 2) which shows that sample is composed of γ-spinel, YAG, and Al_2O_3.

Thermodynamic calculations show that the liquidus of this composition is 1815°C. However, melting was detected in the temperature range of 1850 ± 19° to 1900 ± 19°C. This higher observed value may be due to the fact that the sample temperature was monitored outside the molybdenum tube. Similar discrepancies were observed in all of the samples. As a result, γ-spinel and liquid were present at 1850 ± 19°C in Fig. 2 while γ-spinel should start solidifying at 1815°C according to the thermodynamic calculations. Figure 10 shows that by cooling the melt, γ-spinel first starts to crystallize followed by the precipitation of YAG and Al_2O_3 and this is consistent with the diffraction data obtained during cooling. It can be seen from this figure that as the temperature decreases, the proportion of γ-spinel phase decreases until it decomposes at around 1550°C to give Al_2O_3 and AlN. This agrees with Fig. 3, where AlN peaks are observed at 1400°C and result from the decomposition of γ-spinel. Moreover, around 1800°C the proportion of solids increases rapidly over a narrow temperature range. This means that the composition is sensitive to small changes in temperature.

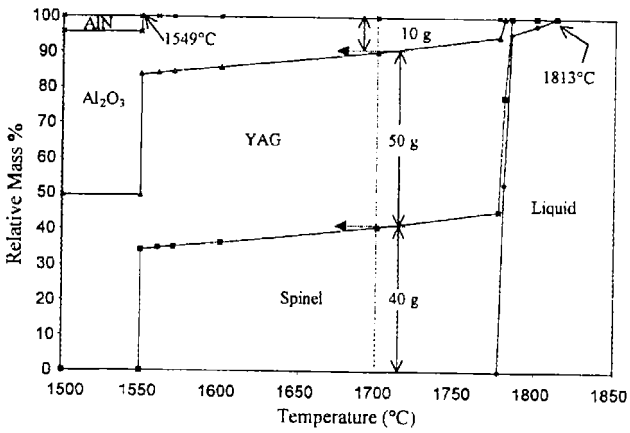

Fig. 10. Phase assemblage diagram of composition 3 (24 mol% AlN, 70 mol% Al_2O_3, and 6 mol% Y_2O_3).

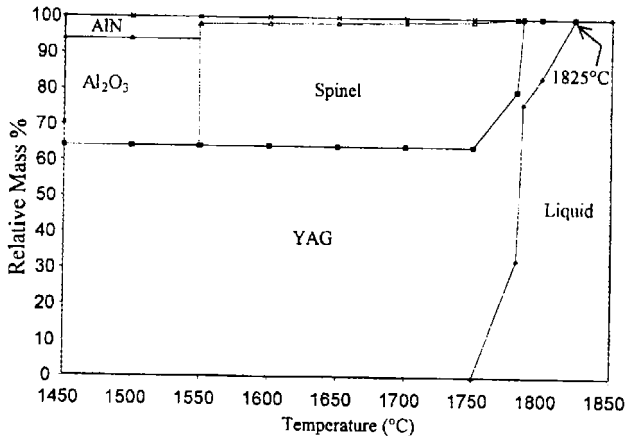

Fig. 11. Neutron diffractograms during heating of composition 5 (33 mol% AlN, 20 mol% Al_2O_3, and 47 mol% Y_2O_3).

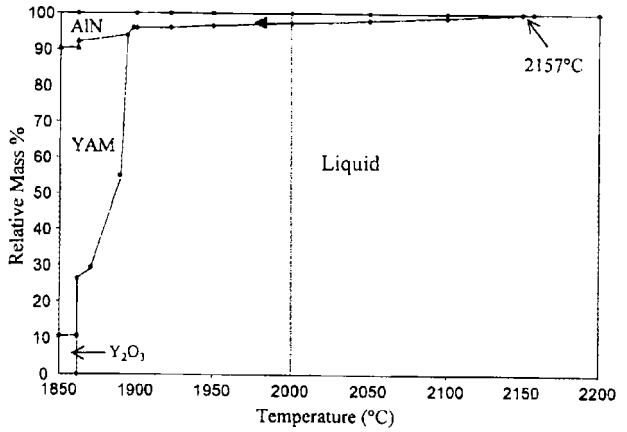

Fig. 13. Phase assemblage diagram of composition 5 (33 mol% AlN, 20 mol% Al_2O_3, and 47 mol% Y_2O_3).

Thermodynamic modeling shows that γ-spinel forms through the reaction between AlN and Al_2O_3 at a temperature higher than 1550°C, whereas the neutron diffraction experiments show incomplete reaction at around 1600°C. However, the experimental results agree with the work of Willems *et al.*, who found that the reaction rate between AlN and Al_2O_3 to produce γ-spinel is sluggish at temperatures below 1750°C.[19] Cheng *et al.*[20] also observed incomplete reaction between Al_2O_3 and AlN at 1650°C for 6 h. They noticed an increase of γ-spinel content with increasing time from 60 min to 6 h. Moreover, Yawei *et al.*[21] concluded that it is difficult to produce γ-spinel by reaction sintering below 1650°C.

The phase assemblage versus temperature of composition 2 is presented in Fig. 11. It can be seen that the liquidus temperature of this composition is 1825°C, whereas according to the neutron diffraction results this composition melted between 1850 ± 19° and 1900 ± 19°C. This difference is attributed to temperature measurement discrepancies, as discussed before. When cooling this composition from its melt, calculations predict that YAG solidifies first, followed by γ-spinel. This is consistent with the neutron diffraction results for the cooling of this composition and shown in Fig. 5.

Thermodynamic calculations also show that γ-spinel decomposes completely at around 1500°C. At room temperature, 100 g of overall material should consist of 64 g of YAG, 6 g of AlN, and 30 g of Al_2O_3. However, diffraction data acquired during cooling indicated that decomposition of the γ-spinel starts below 1400°C and is incomplete on reaching room temperature due to the high cooling rate (25°C/min), with the retention of residual γ-spinel. Nevertheless, this agrees with Yawei *et al.*'s[21] findings, where a sample with high γ-spinel content was annealed in flowing nitrogen gas at 1550°C for 3 h after reaction at 1800°C and was found to contain AlN, Al_2O_3, and γ-spinel, which were retained down to room temperature.

Figure 12 is the phase assemblage for composition 3. It can be seen that the calculated liquidus for this composition is 2030°C. This agrees well with the results of neutron diffraction, where the sample was still partially crystalline at 2000°C, showing that complete melting takes place at higher temperature. From this figure, γ-spinel starts precipitating followed by YAG at around 1800°C. This is consistent with the neutron diffraction patterns collected during cooling and shown in Fig. 7. γ-Spinel was the only solid phase present down to 1850°C. YAG then began to precipitate below 1850°C but above 1600°C. At 1600°C, 100 g of the overall material consists of 75 g of γ-spinel and 25 g of YAG. This is consistent with the pattern collected at 1600°C during cooling and shown in Fig. 7, which indicates that this sample is composed of γ-spinel and YAG.

Thermodynamic calculations show that γ-spinel decomposes completely below 1500°C to Al_2O_3 and AlN for this composition, whereas the experimental results in Fig. 7 show only partial decomposition occurring between 1200° and 1600°C. This is, perhaps, due to the high cooling rate of around 25°C/min.

Figure 14 is calculated for composition 5 from the thermodynamic database of the AlN–Al_2O_3–Y_2O_3 system. Although this composition has a relatively high liquidus temperature of 2157°C, liquid starts forming at 1861°C, as can be seen from this figure. Cooling a sample of this composition from its melt shows that the major phase will be the liquid down to 1898°C. Below this temperature the amount of solid increases rapidly. For instance, 100 g of this sample will be composed of 97 g of liquid and 3 g of AlN at 2000°C. This agrees with the neutron diffraction pattern collected at this temperature, where only AlN peaks were observed. This figure shows that Y_2O_3 starts to recrystallize below 1900°C and is consistent with the neutron diffraction patterns collected during cooling between 1900° and 1850°C. At room temperature, 100 g of this sample will be composed of 10 g of AlN, 78 g of YAM, and 12 g of Y_2O_3. The room-temperature diffraction pattern of Fig. 8 shows that these three phases coexist with strong peaks of YAM, confirming the thermodynamic calculations.

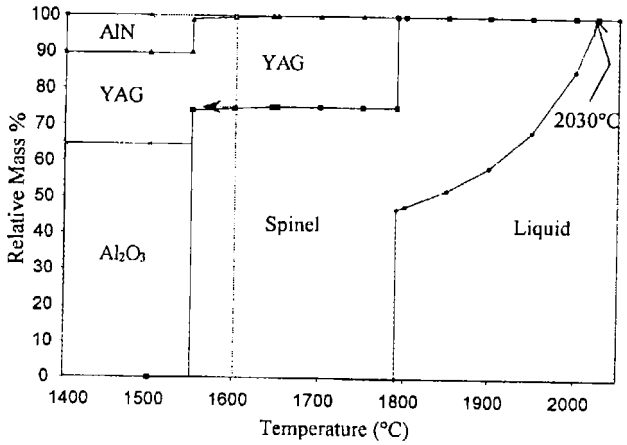

Fig. 12. Neutron diffractograms during cooling of composition 5 (33 mol% AlN, 20 mol% Al_2O_3, and 47 mol% Y_2O_3).

V. Conclusions

(1) High-temperature neutron diffractometry has permitted real time measurement of the reactions involved in the AlN–Al_2O_3–Y_2O_3 ternary system, especially to determine the temperature range for each reaction, which would have been difficult to establish by any other means.

(2) Thermodynamic calculations of AlN–Al_2O_3–Y_2O_3 generally agree well with these experimental results. The difference between the measured temperature and the ones resulting from the phase equilibria modeling, in most of the temperature ranges studied, are within the uncertainty in the thermocouple measurement.

(3) There is no reaction between AlN and YAG, YAP, YAM, or Y_2O_3, which supports the thermodynamic findings.

(4) Some discrepancy between experimental results and the thermodynamic calculations of γ-spinel decomposition temperature was encountered. However, slow reaction and decomposition kinetics of spinel and critical thermodynamic properties have been reported previously and are also corroborated in this study.

References

[1]O. N. Grigoriev, S. M. Kushnerenko, K. A. Plotnikov, and W. Kreher, "Seperation of Internal Strains and Lattice Distortion Caused by Oxygen Impurities in Aluminum Nitride," *Adv. X-ray Anal.*, **38**, 479–87 (1995).

[2]M. Medraj, M. Entezarian, and R. A. L. Drew, "Wettability of Al_2O_3–Y_2O_3 Compounds on Aluminum Nitride and Their Role in Sintering"; pp. 307–12 *Sintering Science and Technology*, Proceedings of the 2nd Sintering '99 Conference (State Collage, PA). Pennsylvania State University, State College, PA, 2000.

[3]N. H. Kim, K. Komeya, and T. Meguro, "Effect of Al_2O_3 Addition on Phase Reaction of AlN–Y_2O_3 System," *J. Mater. Sci*, **31** [6] 1603–608 (1996).

[4]I. C. Huseby and C. F. Bobik, "High Thermal Conductivity Aluminum Nitride Ceramic Body," U.S. Pat. No. 4 547 471, 1985.

[5]J. C. Schuster, "Phase Diagrams Relevant for Sintering Aluminum Nitride Based Ceramics," *Rev. Chim. Miner.*, **6** [24] 676–86 (1987).

[6]W. Y. Sun, Z. K. Huang, T. Y. Tien, and T. S. Yen, "Phase Relationships in the System Y–Al–O–N," *Mater. Lett.*, **3–4** [11] 67–69 (1991).

[7]N. H. Kim, K. Komeya, and T. Meguro, "Effect of Al_2O_3 Addition on Phase Reaction of AlN–Y_2O_3 System," *J. Mater. Sci.*, **31** [6] 1603–608 (1996).

[8]F. Bocy, L. Cao, K. A. Khor, and A. Tok, "Phase Reaction and Sintering Behavior of a Al_2O_3–20 wt% AlN–5 wt% Y_2O_3 System," *Acta Mater.*, **16** [49] 3117–27 (2001).

[9]M. Hoch, "Calculation of Ternary, Quaternary, and Higher-Order Phase Diagrams from Binary Diagrams and Binary Thermodynamic Data," *J. Phase Equilib.*, **14** [6] 710–17 (1993).

[10]M. Medraj, W. T. Thompson, and R. A. L. Drew, "Thermodynamic Modeling of AlN–Al_2O_3–Y_2O_3 System," *Can. Metall. Q.*, in press.

[11]R. E. Lochman (ed.), *Characterization of Ceramics*. Butterworth-Heinemann, Boston, MA, 1993.

[12]L. G. D'yachkov, L. A. Zhilyakov, and A. V. Kostanovskii, "Melting of Aluminum Nitride at Atmospheric Nitrogen Pressure," *Tech. Phys.*, **45** [7] 928–30 (2000).

[13]H. Sawada, "Residual Electron Density Study of α-Aluminum Oxide Through Refinement of Experimental Atomic Scattering Factors," *Mater. Res. Bull.*, **29** [2] 127–33 (1994).

[14]M. Faucher, "Refinement of the Y_2O_3 Structure at 77 K," *Acta Crystall., Sect. B*, **12** [B36] 3209–11 (1980).

[15]R. S. Hay, "Phase Transformation and Microstructure Evolution in Sol-Gel Derived Yttria–Alumina Garnet Films," *J. Mater. Res.*, **3** [8] 578–604 (1993).

[16]T. Hahn (ed.), *International Tables for Crystallography:* Vol. A, *Space Group Symmetry*, 3rd Ed. Kluwer Academic Publishers, Dordrecht, Netherlands, 1992.

[17]H. X. Willems, G. De With, and R. Metselaar, "Neutron Diffraction of γ-Aluminum Oxynitride," *J. Mater. Sci. Lett.*, **18** [12] 1470–72 (1993).

[18]H. Yamane, M. Omori, and T. Hirai, "Thermogravity and Rietveld Analysis for the High-Temperature X-ray Powder Diffraction Pattern of $Y_4Al_2O_9$," *J. Mater. Sci. Lett.*, 7 [14] 470–73 (1995).

[19]H. X. Willems, M. M. R. Hendrix, G. With, and R. Metselaar, "Thermodynamics of Alon: II. Phase Relations," *J. Eur. Ceram. Soc.*, **4** [10] 339–46 (1992).

[20]J. Cheng, D. Agrawal, and R. Roy, "Microwave Synthesis of Aluminum Oxynitride (ALON)," *J. Mater. Sci. Lett.*, [18] 1989–90 (1999).

[21]L. Yawei, L. Nan, and Y. Runzhang, "The Formation and Stability of γ-Aluminum Oxynitride Spinel in the Carbothermal Reduction and Reaction Sintering Processes," *J. Mater. Sci.*, **4** [32] 979–82 (1997). □